

Observations of Comet P/2003 T12 = 2012 A3 (*SOHO*) at large phase angle in *STEREO-B*

M.-T. Hui[★]

Guangzhou, China

Accepted 2013 September 3. Received 2013 September 3; in original form 2013 July 23

ABSTRACT

Comet P/2003 T12 = 2012 A3 (*SOHO*) was observed by the satellite *STEREO-B* during the period 2012 January 13–27. During its apparition, it ventured into the highest phase angle ever observed for a comet, and the forward-scattering enhancement in brightness was marked, as large as ~ 8.5 mag. Therefore, it provided a precious opportunity to examine the compound Henyey–Greenstein (HG) comet–dust light-scattering model and it also offered valuable polarization data under an unprecedented observing geometry. Our analysis reveals that the compound HG model fits the observations very well until the phase angle exceeds $\sim 173^\circ$, where the brightness surge of the comet was obviously steeper than the prediction by the model. We have found that the reason for the greater steepness cannot be explained by contaminations from the proximal tail. Instead, the model of Mie spheres with radii greater than $1\ \mu\text{m}$, having a power-law distribution of power index ~ 3 , matches the observation very well, providing a best-fitting complex refractive index $\mu = 1.38 + i0.006$. The dust size was found to be consistent with the analysis of the comet’s syndyne lines. The debiased polarization of the coma was ~ 0 per cent in the phase angle range from $172^\circ.9$ to $177^\circ.6$. No convincing evidence of temporal variation of the polarization was detected.

Key words: methods: data analysis – techniques: photometric – techniques: polarimetric – comets: individual: P/2003 T12 = 2012 A3 (*SOHO*).

1 INTRODUCTION

The short-periodic comet P/2003 T12 = 2012 A3 (*SOHO*) was first discovered by J. Danaher in images taken by the LASCO C3 telescope of the *Solar and Heliospheric Observatory* (*SOHO*) on 2003 October 9.¹ There were 71 observations spanning 3 d, measured by K. Battams, that led to a parabolic solution in MPEC 2004-K33, designated as C/2003 T12 (*SOHO*). However, B. G. Marsden suggested that the possibility of this being a short-periodic comet with a smaller perihelion distance could not be excluded (Marsden, Kisala & Battams 2004). On 2012 January 19, A. Watson reported a bright unknown comet retreating away from the Sun in the fields of view (FOVs) of *STEREO-B*’s HI-1 images from 2012 January 16. Later, W. T. Thompson managed to trace it back to the COR-2 images. We have conducted brief astrometric and photometric measurements of the comet in all total brightness COR-2 images and in the available HI-1 images in *ASTROMETRICA*, to which R. Kracht added space vectors and obtained a link between the comet and C/2003 T12.² On 2012 January 29, there was an official announcement of the linkage

P/2003 T12 = 2012 A3 (*SOHO*) (hereafter P/2003 T12) in MPEC 2012-B96 (Williams & Battams 2012). Qualitatively, during the measurements of the comet in the COR-2 and HI-1 images, we have clearly noticed a strong brightness surge of the coma, which came to a climax around the time when the comet was apparently closest to the Sun in the FOV of the COR-2 telescope. Despite the fact that *ASTROMETRICA* does not perform photometry in a critically accurate manner, the photometric data have quantitatively confirmed the strong brightness enhancement. In the following analysis, the maximum phase angle of the comet observed was, astonishingly, found to be as large as $177^\circ.6$. Prior to the measurements of these observations, the largest phase angles at which the brightness of a comet and polarization were quantitatively measured were 167° and 157° , respectively (96P/Machholz 1; Grynko, Jockers & Schwenn 2004). In this paper, we have endeavoured to analyse the phase function and polarization of Comet P/2003 T12 from the COR-2 and HI-1 telescopes of *STEREO-B*.

2 OBSERVATIONS

2.1 Overview of *STEREO*

The *Solar Terrestrial Relations Observatory* (*STEREO*) mission consists of two nearly identical spacecrafts, each in an Earth-like

[★]E-mail: wentapachacoti@gmail.com

¹ http://sungrazer.nrl.navy.mil/index.php?p=tables/comets_other

² See messages at <http://tech.groups.yahoo.com/group/stereohunter/message/1665>.

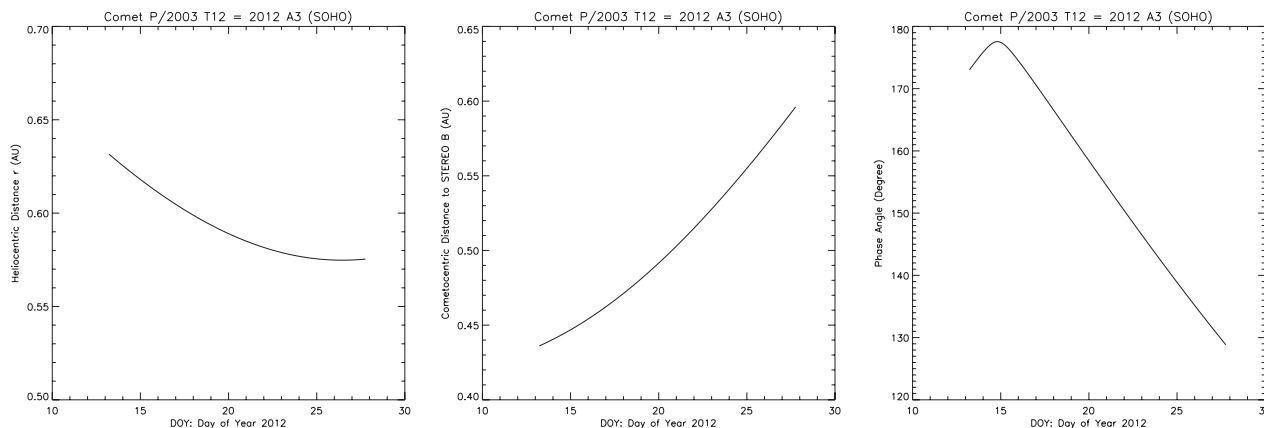


Figure 1. Observing geometry of Comet P/2003 T12 from the perspective of *STEREO-B*.

heliocentric orbit, one ahead of the Earth (*STEREO-A*) and the other behind the Earth (*STEREO-B*). However, they drift with respect to the Earth in opposite directions annually around the Sun. The mission aims to study coronal mass ejections in a stereoscopic manner (Kaiser et al. 2008). *STEREO*'s Sun Earth Connection Coronal and Heliospheric Investigation (SECCHI) instrument suite carries several cameras, including an extreme ultraviolet imager (EUVI), two coronagraphs (COR-1 and COR-2), two heliospheric imagers (HI-1 and HI-2) and a guide telescope (Howard et al. 2008). Only two of the instruments (i.e. COR-2 and HI-1) are related to this paper so the other instruments will simply be ignored.

COR-2 observes an annular FOV, in a range around the Sun from 2.5 to 15 R_{\odot} , whose spectral filter transmits from 650 to 750 nm (FWHM). The polarizer is always in the beam so only polarized images can be obtained. The CCD detector is 2048×2048 pixel² in size. There are two observation modes: (i) a standard sequence consisting of three individual images at -60° , 0° and $+60^{\circ}$; (ii) a total brightness image obtained by summing two images at 0° and 90° (Howard et al. 2008). For the COR-2 images that observed Comet P/2003 T12, all of the total brightness images are in 1×1 binned mode, whereas the majority of the polarized images are binned 2×2 , resulting in final images that are 1024×1024 pixel², with exception of 27 binned 1×1 images from 2012 January 16. One total brightness image was obtained every 30 min, whereas one polarized image was obtained every 60 min. The angular pixel scale of full-resolution COR-2 images is 14.7 arcsec pixel⁻¹, and the binned 2×2 images are double this value.

HI-1 has a square FOV and monitors regions along the ecliptic plane extending from around 4° to 24° elongation, with the angular FOV around 20° . Each HI-1 image consists of 30 separate images of 40-s duration, taken over a period of 30 min and summed onboard; one image is read out every 40 min (Eyles et al. 2009). The CCD detector is 2048×2048 pixel² in size but is binned 2×2 onboard, resulting in an angular size of around 72 arcsec pixel⁻¹ for the 1024×1024 images (Howard et al. 2008). The convolution of the optics transmission with the CCD quantum efficiency yields the overall instrument response, comprised of the major spectral bandpass from 630 to 730 nm (Eyles et al. 2009), along with two leaks ranging from around 300–450 and 900–1000 nm, respectively (Bewsher et al. 2010, fig. 6b).

2.2 Orbit of Comet P/2003 T12 and available *STEREO* data

The final version of the orbital solution with 62 observations spanning from 2003 October 9 to 2012 March 4 for Comet P/2003 T12

was published in MPEC 2012-S31.³ Despite the fact that the comet apparently passed very close to the Sun from the perspective of *STEREO-B*, it is not a Sun-grazing comet ($q = 0.5748$ au). It orbits around the Sun in a low-inclined ($i = 11^{\circ}.47$) elliptical orbit, with an eccentricity $e = 0.78$ in an orbital period $P = 4.12$ yr. The comet passed perihelion at around 11 UT on 2012 January 26. The comet first entered into the FOV of COR-2 at around 5 UT on 2012 January 13. It took the comet more than 3 d and 5 h to complete the transit of the FOV. Unfortunately, because the region monitored by COR-2 and HI-1 is not completely overlapping, the comet was unobservable for around 6 h after moving out of the FOV of COR-2, before it appeared in the HI-1 image from around 17 UT on 2012 January 16. The comet retreated outside the FOV of HI-1 at around 19 UT on 2012 January 27. During the observed period, overall, 231 polarized COR-2 images, 155 total brightness COR-2 images and 394 HI-1 images were useful for measurements. The phase angle increased to the maximum $177^{\circ}.6$ at around 19 UT on 2012 January 14, and thenceforth slowly declined to $128^{\circ}.8$, before it receded from the FOV of HI-1. However, the distance between the comet and *STEREO-B* steadily increased from 0.44 au at first to 0.60 au finally (Fig. 1). Fig. 2 shows the trajectory of the comet recorded by COR-2 and HI-1.

2.3 Ground-based observations

During its apparition in 2012, Comet P/2003 T12 remained in poor elongations from the Sun all the time post-perihelion from a ground-based perspective. The first successful ground-based observation came from H. Sato on 2012 January, 30.06 UT, remotely taken from H06 (Sato & Williams 2012). Overall, 49 ground-based observations of the comet were gathered from Minor Planet Electronic Circulars, spanning from 2012 January 30 to 2012 March 4. However, only 22 of these have photometric measurements. Unfortunately, there was not much information about the ground-based photometry (e.g. photometric aperture sizes). Moreover, it might well be that these measurements might have been compared to very different comparison star catalogues. Taking these negative facts into consideration, which are highly likely to introduce large errors, we have assumed that the data are all in the *R* band in this analysis. The phase angle of the comet was lingering between 62° and 77° from the ground-based perspective, and therefore these photometric data would not be influenced

³ <http://www.minorplanetcenter.net/iau/mpec/K12/K12S31.html>

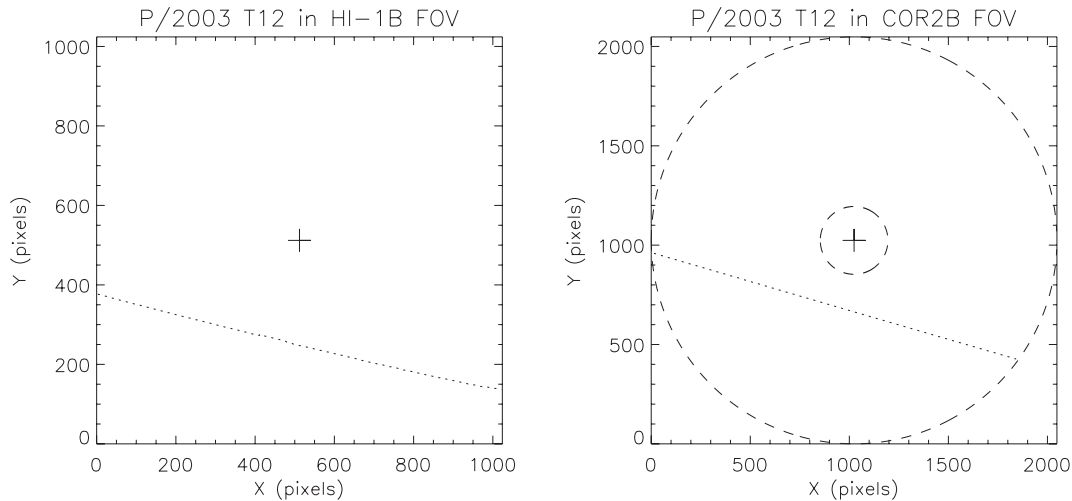


Figure 2. Trajectory of Comet P/2003 T12 in the FOVs of COR-2 and HI-1 of *STEREO-B*. The comet moved from left to right in both FOVs. The annular region between the two dashed circles in the right panel shows the observable FOV of COR-2. Regions within the smaller circle or outside the larger circle are blocked and unobservable.

by the forward-scattering effect. These photometric data would therefore be employed to analyse the baseline light curve of the comet.

2.4 Image calibration

We used only level-0.5 images, which are publicly available from the *STEREO* Science Center for measurements.⁴ These images are raw, uncalibrated instrument images processed from the spacecraft telemetry into FITS file format. The images are in units of DN (digital number or counts). The calibration work was performed in IDL with SECCHI_PREP under the SolarSoftWare library. The routine basically subtracts the offset bias for each image, normalizes the corresponding exposure time and finally multiplies the bias-subtracted and exposure-normalized images by the vignetting function, either for COR-2 or for HI-1. It has to apply the correction for shutterless readout of the HI-1 camera specifically, before normalizing the exposure time (Eyles et al. 2009). We did not apply the correction for geometry distortion of the COR-2 images, otherwise the correction would interpolate between pixels and some low signal-to-noise (S/N) field stars could be smeared out by visual inspection. The calibrated images are dominated by the F-corona and therefore it is necessary to remove the background. Median background images must be constructed. Different methods were applied for the COR-2 and HI-1 images. For COR-2 images, because the stars are not dense in the background, we employed the method described by Knight et al. (2010) for constructing median background images from calibrated *SOHO/LASCO* C2 and C3 images. For HI-1 images, however, because the pixel scale is very large, there are always myriads of stars in any of the images, making the aforementioned method, which was applied to COR-2 images, inapplicable. Instead, a median background image was constructed from the daily sequence. The calibrated images were subtracted by the corresponding background images, yielding the final processed images to be measured.

2.5 Aperture photometry

Circular apertures centred on the optocentre of Comet P/2003 T12 were exploited in order to calculate the aperture photometry using the APER routine. The optocentre of the comet was first found by the CNTRD routine. In the rare case where CNTRD failed to do the work, GCNTRD was applied instead.⁵ For photometric measurements with total brightness COR-2 and HI-1 images, the sizes of the apertures were chosen to be large enough to encompass the signal from the comet as much as possible. Meanwhile, however, they had to minimize contaminations from background signals. Repeated tests revealed that a circular aperture of 8 pixels (2.0 arcmin) in radius for full-resolution 2048×2048 total brightness COR-2 images and 5.5 pixels (6.4 arcmin) in radius for HI-1 images were optimal. For polarimetric measurements with polarized COR-2 images, however, it was found that the aperture size could not be as large as 8 pixels in radius with full-resolution images, otherwise the resulting polarization data would have extremely high uncertainty. The size of the aperture was selected to be 4 pixels in radius instead, and as a result the S/N increased. The 2×2 binned COR-2 images had halved aperture sizes accordingly. In case any contaminant (i.e. commonly, background stars and cosmic rays) was in the vicinity of the coma, which might affect photometry and exaggerate the actual flux, there are two strategies applicable for HI-1 and COR-2 images, respectively. For full-resolution COR-2 images, every pixel occupied by the star contaminant was manually substituted by an artificial median background constructed within a square window of 11×11 pixel², centred on that pixel. The dimensions were 5×5 for 2×2 binned COR-2 images. The dimensions for constructing an artificial median background were found to be trivial unless too small a size was applied. There were nine total brightness and three polarized images with which the contaminant removal was performed. For HI-1 images, because the background contaminants hardly ceased, the star removal routine for HI images HI_REMOVE_STARFIELD under the SolarSoftWare library was applied for removing background sources brighter than

⁴ http://stereo-ssc.nascom.nasa.gov/data/ins_data/secchi/L0/

⁵ APER, CNTRD and GCNTRD are all a part of the IDL Astronomy Library, available from <http://idlastro.gsfc.nasa.gov/>.

the comet. We have randomly selected a great number of HI-1 images in which background stars fall into the photometric aperture but remain apparently separated with the comet. Using appropriate parameters, the routine successfully removed only contaminants while the flux of the comet remained unharmed. The photometric results were consistent with measurements with images close in time, in which the comet was free from any significant contaminant. Thus, this proved that this routine would not affect the reliability of photometry. In case the comet apparently adjoined the contaminant, there was no measure taken with these images and they were discarded directly. It was very frequent, almost unavoidable, that faint contaminants fell into the aperture because of the large angular image scale of the HI-1 images, in which case these data were still applied, and the photometric data would be too scarce otherwise. Nevertheless, this introduces more scatter, but the large number of images yields a relatively smooth envelope of the data.

For photometry, the measured fluxes in DN s^{-1} were translated to apparent magnitude using

$$m = ZP - 2.5 \log F, \quad (1)$$

where m is the apparent magnitude, ZP is the zero-point of the image and F is the integrated flux of the comet in DN s^{-1} . The STEREO team has calculated the zero-point for the HI-1 images (Bewsher et al. 2010). However, the zero-point is not yet available for polarized and total brightness COR-2 images. By selecting 1289 observations of 12 background stars, whose magnitudes range from around 3.2 to around 8.5 in the R -band Naval Observatories Merged Astrometric Data set star catalogue (NOMAD), all in the lower part of the total brightness COR-2 images from 2012 January 13 to 16, by folding the stellar spectra with the instrument response provided by A. Vourlidas (private communication), we obtained the zero-point of the total brightness COR-2 images as $ZP = 12.664 \pm 0.092$ for F in DN s^{-1} . After converting F into mean solar brightness (MSB), we found that this value was similar to that determined by M. M. Knight (private communication). It is desirable, however, to obtain the value in a more rigorous way, by measuring many more comparison stars in the COR-2 images. For polarimetry, we used the following equation for calculating the polarization of the comet:

$$P = \frac{pB}{B}. \quad (2)$$

Here, P is the polarization degree, pB is the brightness of the polarized flux and B is the brightness of all the flux. We have assumed that all of the polarized light from the coma was linear, because the majority of the polarimetric observations of different comets only reveal linear polarization, whilst hitherto circular polarization has been reliably detected for seven comets only: 1P/Halley, 8P/Tuttle, 9P/Tempel 1, 73P/Schwassmann–Wachmann 3, C/1995 O1 (Hale–Bopp), D/1999 S4 (LINEAR) and C/2001 Q4 (NEAT).⁶ Therefore, we can calculate pB from

$$pB = \frac{4}{3} \left[\left(\sum_{i=1}^{n=3} F_i \right)^2 - 3 \sum_{i \neq j} F_i F_j \right]^{1/2}, \quad (3)$$

where F_1 , F_2 and F_3 represent fluxes of the comet in 0° , $+60^\circ$ and -60° polarized images, respectively. We obtain B from

$$B = \frac{2}{3} \sum_{i=1}^{n=3} F_i. \quad (4)$$

2.6 Estimating the errors

The total error of the magnitudes and the fluxes is a combination of the errors from varieties of components that were involved in the calculation of the magnitude and flux, based on the propagation of uncertainty. We have assumed that the statistical uncertainty in the CCD detector counts and errors from the zero-points of the HI-1 and COR-2 images are dominant. The uncertainty of the zero-point for the HI-1 images was estimated to be ~ 0.05 mag to account for the error from the calculated flat-field and the potential long-term evolution of the sensitivity of the detector, although no sign of degradation of the instrument was found (Bewsher, Brown & Eyles 2012). Other errors from parameters for describing the observing geometry (bias, exposure time, etc.) also contribute to the total uncertainty, but we have not included these into our calculations because they are much smaller than the aforementioned estimated errors.

3 RESULTS

3.1 Light curve and phase function

Fig. 3 illustrates the photometric measurement data of all the usable COR-2 and HI-1 images. We can clearly see that the apparent magnitude of Comet P/2003 T12 peaked at around day of year (DOY) = 15 (i.e. 2012 January 15), and then steadily declined, although it was still heading towards perihelion. Because one of the principal targets in this paper is to derive the phase function of the comet, the baseline light curve of the comet must be known. The apparent magnitude data must be corrected for the heliocentric distance of the comet r , along with the comet–spacecraft distance Δ . The methodology is achieved by

$$\begin{aligned} \Phi(\alpha) &= m - 5 \log(\Delta) - 2.5 n \log(r) - m_0 \\ &= H - 2.5 n \log(r) - m_0, \end{aligned} \quad (5)$$

where α is the phase angle, $\Phi(\alpha)$ is the phase function, m is the observed magnitude, m_0 is the absolute magnitude, n is the index of the brightening, typically dependent upon r over a large observing arc, and H is the heliocentric magnitude as defined at $\Delta = 1$ au. If the range of r is limited, and if there is no occurrence of a large-scale sudden change of cometary activities (i.e. outbursts, fragmentations, disintegrations, etc.), it will normally be safe to apply a constant n .

Fig. 4 shows the heliocentric magnitude of Comet P/2003 T12 observed by COR-2 and HI-1 of STEREO-B as a function of $\log(r)$. It is more obvious that the brightness of the comet culminated when $\log(r) = -0.208$, rather than at perihelion. Also displayed is the existence of a small discontinuity between the COR-2 and HI-1 data, because the comet appears brighter in HI-1 than predicted by the trend of COR-2 observations. While the possibility of a sudden outburst during the 6-h unobserved period cannot be ruled out, it is more likely that the magnitude difference should be attributed to the different bandpasses of COR-2 and HI-1. Whilst the major bandpasses of COR-2 and HI-1 are very similar, the blue leak of the HI-1 spectral response should be the most likely factor responsible for

⁶ Poster by Kiselev N., Rosenbush V., 2012, Polarimetry of Comets: Observational Results and Problems, WG1, Warsaw (http://www.polarisation.eu/projectdir/Kiselev_Warsaw_2.pdf).

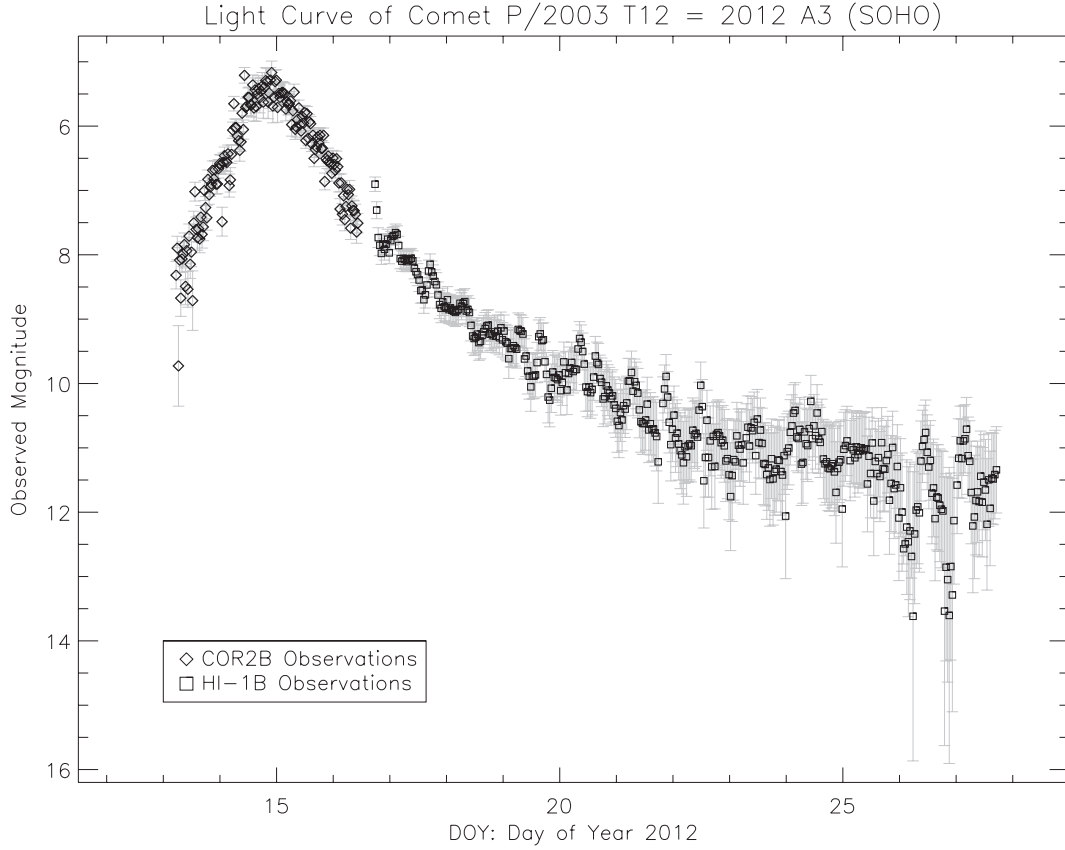


Figure 3. Apparent magnitude of Comet P/2003 T12 as a function of DOY.

the magnitude difference, through which strong gas emission lines, such as CN, C₃ or even Fe I, if there is any, would be transmittable (see Fig. 5). We have estimated that the COR-2–HI-1 magnitude difference is around +0.5, that the HI-1 magnitude of the comet is brighter than the *R*-band magnitude by around −0.1 and that the COR-2 magnitude is fainter than the *R*-band magnitude by around +0.4 (see Section 4.1 for details).

Marcus (2007a) has put forward a compound Henyey–Greenstein (HG) model of the phase function of coma brightness due to dust particles. The model successfully interprets the forward-scattering effect as well as the back-scattering effect. Observations of several comets that suffer from strong forward-scattering brightness enhancement, including several famous bright historical comets and 96P/Machholz 1, C/2004 F4 (Bradfield), C/2006 P1 (McNaught), etc., have been accurately explained by the model (Marcus 2007a, 2007b). It has also been applied to correct the brightness of Kreutz Sun-grazing comets observed by the *SOHO*/LASCO C2 and C3 cameras between 1996 and 2005 (Knight et al. 2010). The compound HG model was given by Marcus (2007a) in the following form:

$$\phi(\alpha) = \frac{\delta_{90}}{1 + \delta_{90}} \left\{ k \left[\frac{1 + g_f^2}{1 + g_f^2 - 2g_f \cos(180^\circ - \alpha)} \right]^{3/2} + (1 - k) \left[\frac{1 + g_b^2}{1 + g_b^2 - 2g_b \cos(180^\circ - \alpha)} \right]^{3/2} + \frac{1}{\delta_{90}} \right\}. \quad (6)$$

Here, $\phi(\alpha)$ is the scattering function, which can be converted into magnitude correction by $\Phi(\alpha) = -2.5 \log[\phi(\alpha)]$, δ_{90} is the dust-to-gas flux ratio of the coma observed at $\alpha = 90^\circ$, k is the partitioning coefficient between forward-scattering and back-scattering, which satisfies $0 \leq k \leq 1$, and g_f and g_b are the forward- and back-scattering asymmetry factors, respectively, which satisfy $0 \leq g_f < 1$ and $-1 < g_b \leq 0$. Comet observations were well fitted to the model with $k = 0.95$, $g_f = 0.9$ and $g_b = -0.6$ (Marcus 2007a). However, the compound HG model has never been examined in the phase angle range that Comet P/2003 T12 achieved in its 2012 apparition observed by *STEREO-B*. Therefore, it is of great interest to compare the model with the observation data.

In order to compare the phase function of the comet against the compound HG model in the unprecedented observed large phase angles, the photometric data from 22 ground-based observations were utilized to derive m_0 and n so that there is no influence from the phase effect. According to the compound HG model, these ground-based observations would be influenced by side-scattering. The dustier the comet is, the larger the magnitude correction will be. If Comet P/2003 T12 had been an extremely dusty comet (i.e. with $\delta_{90} = 10$), the correction would have been $+0.25 \leq \Phi(\alpha) \leq +0.42$ only. For a typical comet with $\delta_{90} = 1$, the correction will be no greater than +0.21. Evidence from the analysis suggests that Comet P/2003 T12 is actually a gassy comet (see Section 4.1 for details). Therefore, the magnitude correction should be even smaller for the ground-based observations and the influence from the side-scattering can thus be ignored, namely $\Phi(\alpha) \approx 0$, in comparison to the errors described in Section 2.3. Additionally, it was presumed that there had been no

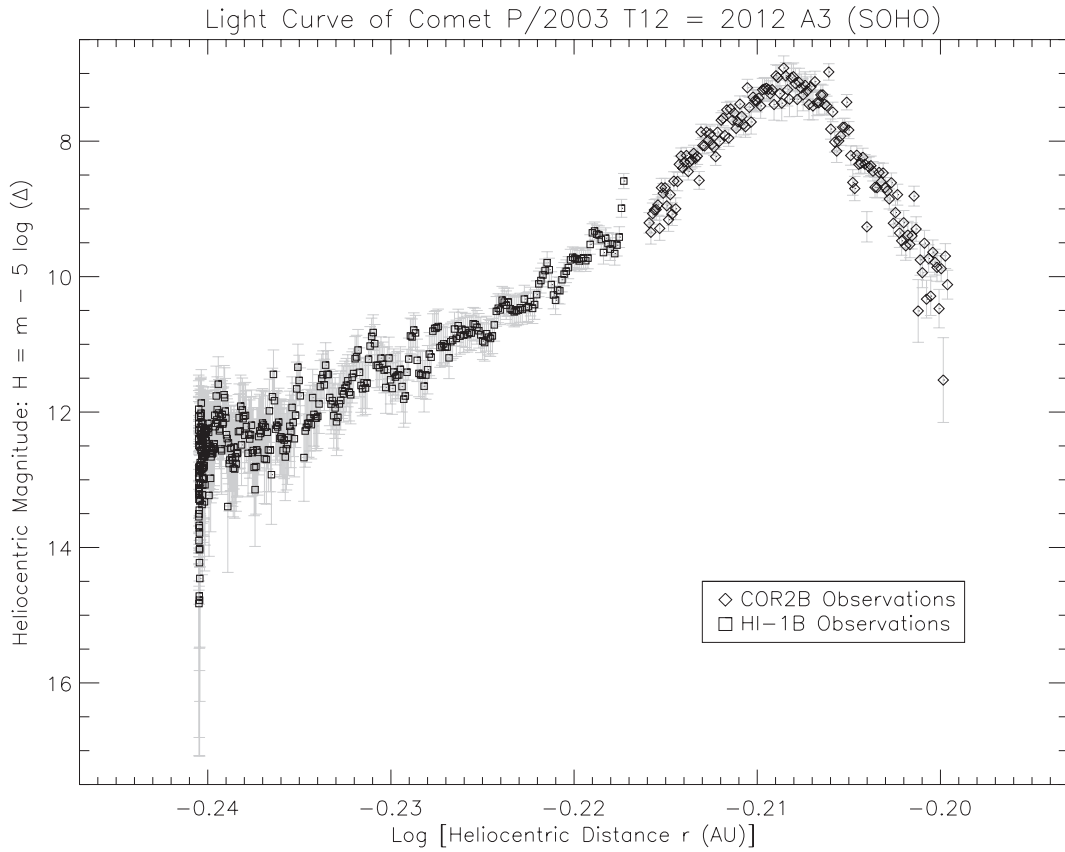


Figure 4. Heliocentric magnitude of the comet as a function of $\log(r)$. Strong non-linearity of the COR-2 data is markedly illustrated.

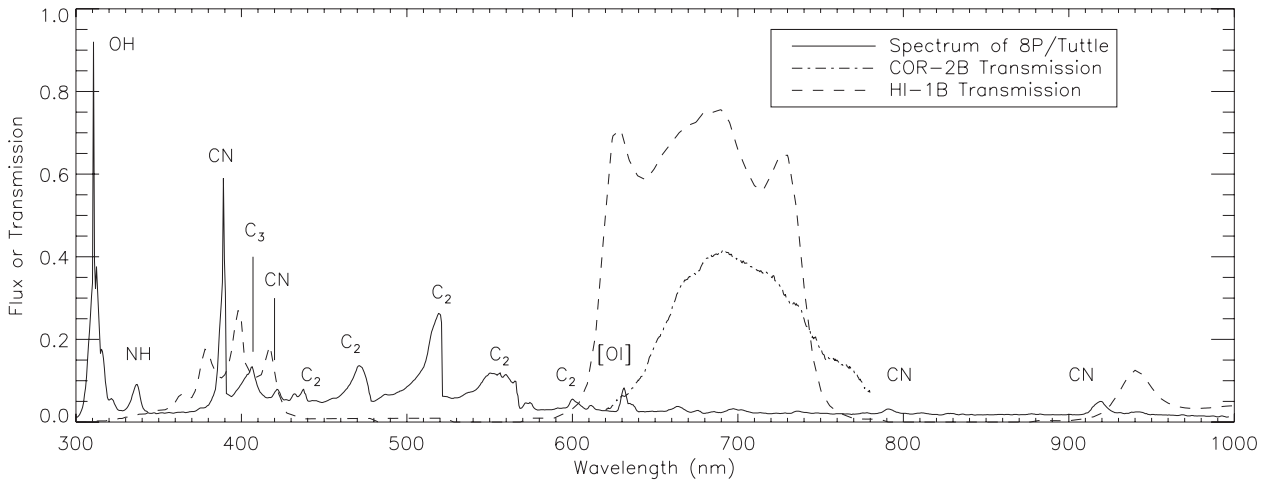


Figure 5. Transmission data from the COR-2 camera of *STEREO-B* (courtesy of A. Vourlidas) and from the HI-1 camera (courtesy of the *STEREO* team, provided by M. M. Knight), along with the spectrum of Comet 8P/Tuttle in its 1980 apparition (courtesy of S. Larson, provided by M. M. Knight). The intensity of the cometary spectrum is in 10^{-6} erg s^{-1} cm^2 \AA str.

occurrence of abnormal activity (i.e. outbursts, sudden fading, etc.) with the comet prior to the first ground-based observation on 2012 January 30 since it included the transit in the FOV of HI-1 late on 2012 January 27. Least-squares linear regression on equation (5) for the ground-based observations yields the following parameters for the baseline light curve: $m_0 = 20.65 \pm 0.18$ and $n = 9.53 \pm 0.44$. However, because the amount of photometric data is far from sufficient, plus the quality and accuracy are unknown, a coarser pair $m_0 = 20.5$ and $n = 10$ were applied in the analysis, which is

consistent with the values adopted by Seiichi Yoshida.⁷ The Jet Propulsion Laboratory (JPL) HORIZONS system calculated $m_0 = 17.1$ for this comet from six observations, with an assumed brightening slope $n = 10$.⁸ We think that the value of m_0 given by

⁷ <http://www.aerith.net/comet/catalog/2003T12/2012.html>

⁸ The two physical parameters can be found by searching for the comet in the JPL Small-Body Data base Browser at <http://ssd.jpl.nasa.gov/sbdb.cgi>.

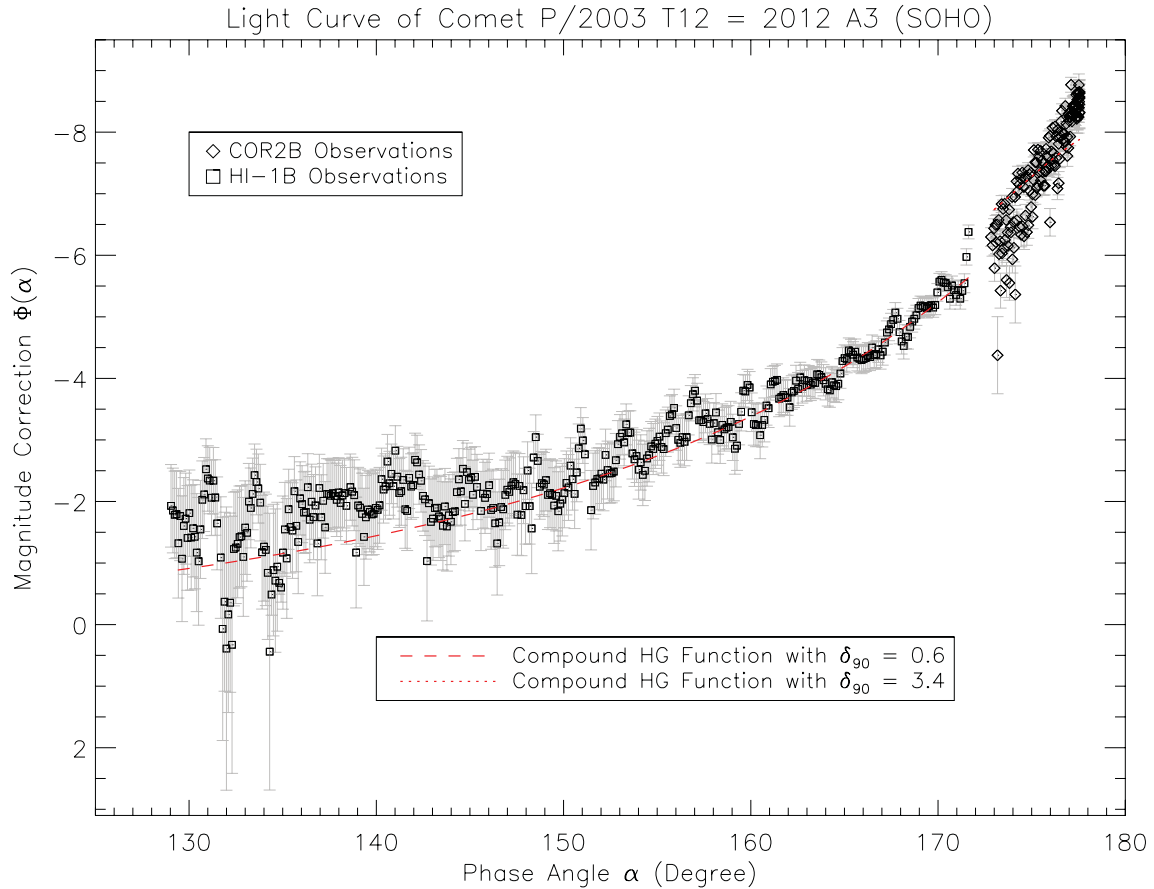


Figure 6. Phase function of the comet observed by *STEREO-B*. The magnitude data are colour-corrected according to the text. Also plotted are the two predictions by the compound HG model for COR-2 and HI-1, respectively.

the JPL is evidently too bright to fit the photometric data of the 22 ground-based observations.

The resulting phase function of the comet versus phase angle is shown in Fig. 6. The marked brightness enhancement as a result of the forward-scattering effect is quantitatively illustrated. The maximum surge was as remarkable as $\Phi \approx -8.5$ mag around the maximum phase angle $\alpha_{\max} = 177.6$. As a comparison, the predictions given by the compound HG model are also plotted in the figure. We have estimated that δ_{90} for HI-1 and COR-2 is ~ 0.6 and ~ 3.4 , respectively (see Section 4.1 for details). The compound HG model fits the HI-1 observations well, although the observations show fluctuations, possibly because of inevitable contamination from nearby star fields. However, in contrast with the HI-1 data, the compound HG model fails to match the trend of the COR-2 observation data with phase angles $\alpha \gtrsim 173^\circ$, but displays a much gentler slope, despite the fact that varying values of δ_{90} have been tested. These are better illustrated in Fig. 7, which is a close-up view of Fig. 6 around the large phase angles.

3.2 Polarization

Because the COR-2 bandpass transmits very little signal of cometary plasma and gas, there is very little influence from non-dust contaminants upon the polarimetric data, so they basically reflect the polarimetric properties of the dust within the coma of Comet P/2003 T12. The photometric measurements of the comet at three polarizer positions 0° , -60° and $+60^\circ$ in COR-2 are presented in

Fig. 8, which shows the same trend of brightness surge around the maximum phase angle on 2012 January 14.9 UT. The polarization degree was calculated using equations (2), (3) and (4), as shown in Fig. 9. The error bars in the plot are mainly attributed to the poor S/N of the comet plus the uncertainty in background determination. The closer the apparent angular distance between the comet and the Sun, the greater the uncertainty is, because of contamination from residuals of the solar corona. Given the large errors, we have followed the method described by Wardle & Kronberg (1974) and have applied debiasing of the polarization data. The data are shown together with the uncorrected polarization in Fig. 9. We have found that the corrected data show $P \sim 0$ throughout $172.9 \leq \alpha \leq 177.6$, and no apparent temporal variation of the polarization was seen. Because of the large uncertainty in the polarimetric data and the relatively small range of phase angles that the observations covered, we were not able to determine a meaningful trigonometric fit to the data. Notwithstanding this, these polarization data are of high value because they are hitherto the largest phase angle polarimetric observations of any comet.

It is worth noting that Kolokolova & Mackowski (2012) computed the polarization of light scattered by large aggregates of diverse structure and porosity in the multisphere T-matrix (MSTM) method, revealing that polarization larger than $\alpha \sim 175^\circ$ should be close to 0, whatever the structure and porosity of the large aggregates. Taking the large errors into account, we think that our measurements have confirmed their theoretical results.

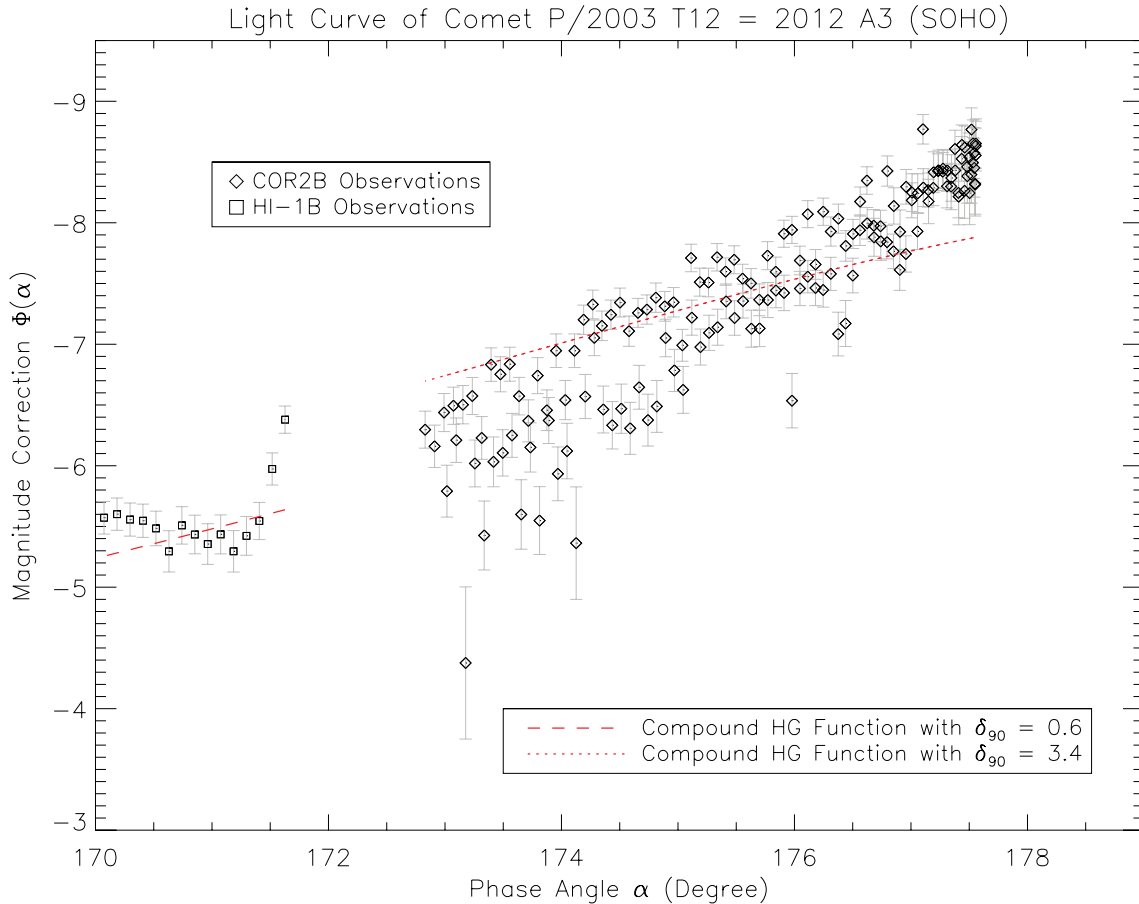


Figure 7. Close-up view of Fig. 6 at large phase angles. The deviation between the slope of the observation data and the trend given by the compound HG model is clearly seen, although some of the data do closely dot around the prediction.

4 DISCUSSION

4.1 Colour of the comet

Comet P/2003 T12 is inferred to be a gassy comet from the fact that it appeared brighter in the HI-1 images than the brightness trend predicted by COR-2 observations, although the possibility of a sudden outburst of the comet during the unobservable gap between COR-2 and HI-1 monitoring coverage cannot be completely ruled out. It is thought that gas emissions transmitting through the blue leak of the HI-1 spectral response contribute to the extra signal, thereby resulting in a brighter magnitude of the comet in the HI-1 images. Observations from the Lowell Observatory around 2012 January 31.08 UT have confirmed this deduction, because the comet displays a bright and large CN coma in the narrow-band CN filtered image, whereas the comet appears tiny with a faint dust tail in the *R*-band image (Knight M. M., private communication). In order to test this, we estimated the predicted flux F using the spectrum-folding technique, which convolves the effective instrumental spectral response with a given spectrum and integrates over the entire spectral range. The following equation is applied in the calculation:

$$F = \int T(\lambda) Q(\lambda) S(\lambda) d\lambda. \quad (7)$$

Here, λ is the wavelength, T is the transmission function of all the optical components encountered with incident photons, Q is the

quantum efficiency of the detector and S is the given spectrum. The flux is then converted into magnitude by

$$m = -2.5 \log \left(\frac{F}{F_0} \right), \quad (8)$$

where F_0 is the intensity of Vega through the instrument. Because the spectrum of Vega is known, F_0 can also be solved by applying equation (7). The spectrum is available within the stellar spectral library of Pickles (1998).

Although comet dust normally appears redder than the Sun, as proved by Jewitt & Meech (1986), we have initially assumed that the spectrum of Comet P/2003 T12 is essentially solar continuum as an approximation. The spectrum was taken from the 1985 Wehrli Standard Extraterrestrial Solar Irradiance Spectrum.⁹ We found that the comet would appear brighter in the COR-2 images than it would in the HI-1 images, by around -0.3 mag, and that it would appear fainter in the HI-1 images than it would in the *R* band, by more than 0.1 mag. Because the spectra of comet dust are normally redder, the comet would appear even brighter in the COR-2 images than in the HI-1 images; however, this obviously contradicts the observation data.

Unfortunately, there has not been any spectroscopic observation of Comet P/2003 T12, and data of cometary spectra are not abundant at small heliocentric distances; in fact, we have not found any

⁹ <http://rredc.nrel.gov/solar/spectra/am0/wehrli1985.new.html>

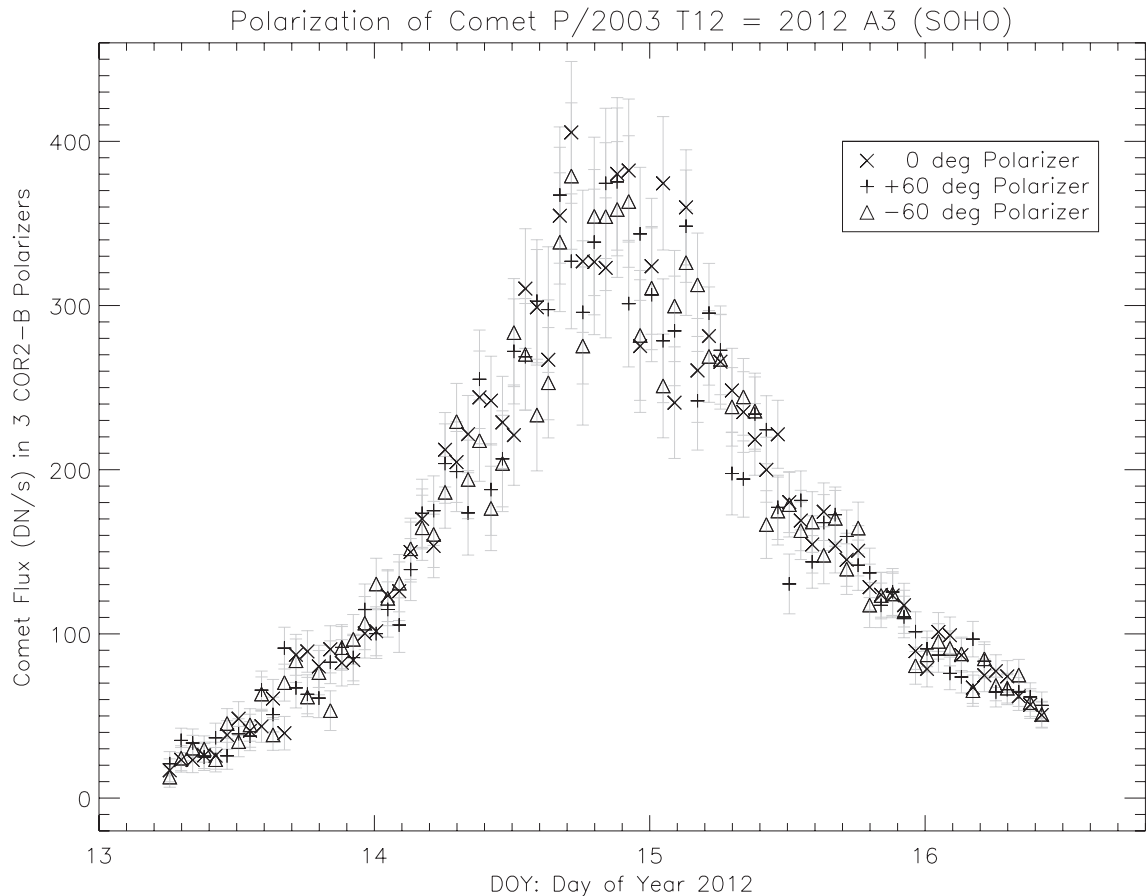


Figure 8. Photometric data in the three different COR-2 polarizers. We can see that the brightness surges followed an almost identical trend. The maximum enhancement in the polarizers coincided with the moment observed by these total brightness images.

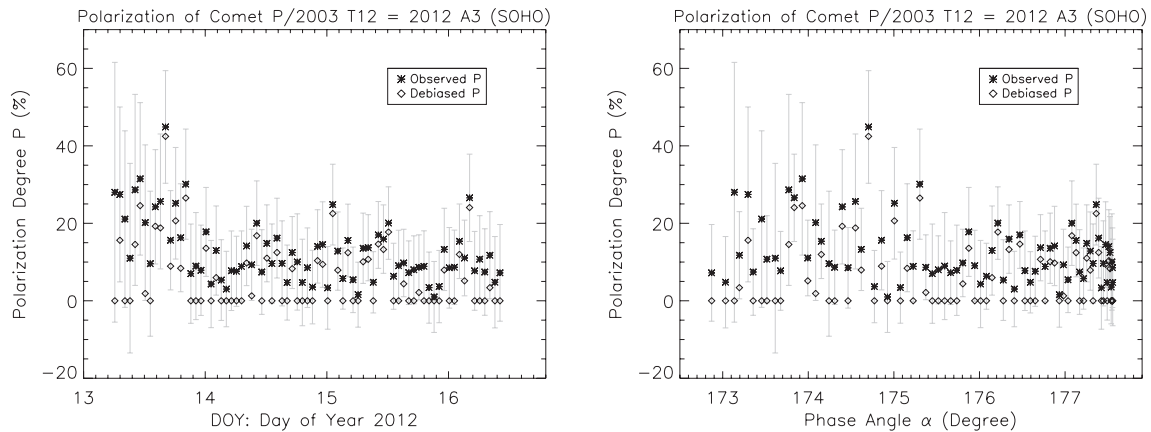


Figure 9. The left panel illustrates polarization degree as a function of time. The right panel illustrates polarization degree as a function of phase angle α . Both the observed and debiased polarization degrees are plotted.

cometary spectra available at the heliocentric distance that P/2003 T12 reached to use for comparison. Thus, we applied the spectrum of Comet 8P/Tuttle observed in the 1980 apparition, spliced together by S. Larson (provided by M. M. Knight) for the estimate as an alternative (see Fig. 5). Because Comet 8P/Tuttle never reaches regions within $r = 1$ au, it is expected that gas emission lines would be much stronger if it had reached a heliocentric distance as small as the distance that Comet P/2003 T12 reached. A rigorous method

to model the spectrum of Comet 8P/Tuttle if it were placed at $r \sim 0.6$ au is to scale the response of emission lines to $r \sim 0.6$ au, taking the g -factors, Swings effect and Greenstein effect into consideration. However, it is likely that the spectrum of Comet P/2003 T12 is dissimilar to the spectrum of Comet 8P/Tuttle because of the diversities in the coma compositions. Therefore, we have only taken the heliocentric distance factor into account and we have modified the spectrum of Comet 8P/Tuttle by amplifying the intensity of the

gas emission by 3.4 times as a coarse simulation. We have found that the resulting magnitude difference between COR-2 and HI-1 matches the observations well. More explicitly, we have found that the comet would appear brighter in the HI-1 images than would it in the R band, by around -0.1 mag, and that it would appear fainter in the COR-2 images than in R band by around $+0.4$ mag. Also, we have estimated the magnitude difference of the comet between the V and R bands to be $V - R \sim -1.1$. For comet dust, $V - R$ is usually around $+0.4$ or larger, because the colour is normally red in comparison to the solar continuum (Jewitt & Meech 1986). We think that the apparent strong bluish hue of the coma can be explained if there are significant gas emission lines in the bandpass. The integrated flux due to gas emission lines was found to be ~ 1.6 times more than the integrated flux due to the solar continuum in the HI-1 camera, whereas the integrated flux due to the solar continuum is ~ 3.4 times more than the integrated flux due to the gas in the COR-2 camera.

Inappropriate photometric zero-points of COR-2 and/or HI-1 images can also explain the COR-2–HI-1 magnitude difference. However, the zero-point of the HI-1 images has been tested by the STEREO team and has been found to be reliable (Bewsher et al. 2012). We have tested, in particular, the accuracy of the zero-point of the total brightness COR-2 images and we think that it should also be accurate. Any revisions of the value will be small so this is unlikely to explain the large colour difference of the comet.

4.2 COR-2 photometric data slope

Fig. 7 shows that the brightness trend of the COR-2 photometric observations of Comet P/2003 T12 is apparently steeper than that of the compound HG model with $\delta_{90} = 10$. It was initially assumed that the neighbouring tail of Comet P/2003 T12 has acted as the contaminant. It is believed that the greater steepness of Comet C/2004 F4 (Bradfield) and of Comet 96P/Machholz observed by SOHO at large phase angles is a result of this projection geometry (Marcus 2007a). Before simulating the potential dust contamination, we examined the COR-2 images closely, and generated synchrones and syndynes of Comet P/2003 T12 from the perspective of STEREO-B. Only a trailing dust tail is discernible in the COR-2 sequence.

The simulation of proximal tail contamination was completed in the following simplified and approximated manner. The tail was assumed to lie in the orbital plane of the comet only. The angle between the antisolar direction and the tail is denoted by χ . It was found that χ would not vary much while the comet was observed by the COR-2 camera, thereby it is approximated as a constant. As the phase angle α increases, more and more signal from the proximal tail will fall into the photometric aperture, scaling as $1/\sin(\chi + \alpha)$. The normalization was set to the first COR-2 observation. We found that only when $\chi \sim 0$ would the corrected slope of the brightness relatively match the trend given by the compound HG model with large δ_{90} . This means that an ion tail of the comet would be responsible for the greater steepness. However, if $\chi \sim 90^\circ$, the correction would be essentially trivial. Yet the comet shows no ion tail in any of the COR-2 images. We stacked several groups of the selected neighbouring 10 images of 2012 January 15, when the brightness of the comet started to decline from the climax, with registration on the comet motion so as to improve the S/N. However, whilst the dust tail becomes brighter and longer than any of the single images, there is still no hint of the ion tail along the antisolar direction, despite the fact that its position angle should be slowly changing from image to image. It is highly unlikely that an invisible ion tail would contribute such a large influence upon

the brightness trend. The explanation given by the proximal tail contamination is therefore denied.

We then applied Mie scattering computation of spheres¹⁰ and compared the results against the COR-2 data. We modelled the particle size distribution in the form

$$n(R) \propto R^{-p}, \quad (9)$$

where $n(R)$ is the number of particles, R is the particle radius and p is the power-law index. Fulle (2004) found that all the comets he analysed had $3 \leq p \leq 4$. The larger p is, the steeper the dust size distribution will be and there will be more concentration in smaller particles. We speculated that the greater steepness of the COR-2 observations was likely to be a result of larger sizes of dust within the coma, and therefore $p = 3$ was applied. The size parameter is defined by

$$x = \frac{2\pi R}{\lambda_{\text{eff}}}, \quad (10)$$

where λ_{eff} is the effective wavelength; we used $\lambda_{\text{eff}} = 0.7 \mu\text{m}$ for the COR-2 camera. In our calculations, we restricted R to be between 1 and $20 \mu\text{m}$, which is equivalent to $9 \lesssim x \lesssim 180$ and an effective dust radius $R_{\text{eff}} \sim 2 \mu\text{m}$ under the condition of $p = 3$. During the experiment, we realized that particles with even greater x posed very little influence upon the result, because their number decreased according to the power-law distribution. However, the presence of smaller particles would significantly decrease the intensity of the surge because of the forward-scattering effect around α_{max} , and would therefore fail to match the observation data. This is also consistent with our computation of the syndyne and synchron models of the trajectory of dust particles (see Fig. 10). The ratio between the solar radiation pressure and the gravity driven by the Sun can be written as

$$\beta = \frac{3Q_{\text{pr}}F_{\odot}}{4\pi cGM_{\odot}\rho_{\text{d}}R}, \quad (11)$$

where F_{\odot} is the mean total solar radiation, Q_{pr} is the dimensionless radiation pressure efficiency, c is the speed of light, G is the gravitational constant, M_{\odot} is the solar mass and ρ_{d} is the density of the dust particles. With the values of constants noted and assuming $Q_{\text{pr}} = 1$ and $\rho_{\text{d}} = 2000 \text{ kg m}^{-3}$, we found $R \geq 1 \mu\text{m}$, consistent with the restriction for Mie scattering computation, because no dust with $\beta > 0.3$ can be seen in Fig. 10. The Mie scattering computation revealed that the best fit of the complex refractive index $\mu = \nu - i\kappa$, where ν and κ are the real and imaginary parts of the refractive index, respectively, was determined to be $\mu = 1.38 + i0.006$ (see Fig. 11).

It is also possible that the greater steepness of the brightness trend of the COR-2 photometric data is a result of intrinsic cometary activities. Asymmetry of the brightness trend pre- α_{max} and post- α_{max} is noticeable because the slope of the pre- α_{max} data is steeper than the slope of the post- α_{max} data. We found that the asymmetry could not be removed by normalizing the two distance factors r and Δ or by applying the heliocentric dependence $n = 10$. It is likely that the dust activities have strengthened, perhaps because of the nucleus rotation or perhaps because we were seeing the seasonal effect. The possibility that the ephemeris of Comet P/2003 T12 is inaccurate by a minute amount, whereby the asymmetry effect was artificially enhanced, is not likely to introduce such a noticeable effect, based

¹⁰ For simplicity, the Mie scattering computation was performed using MIEPLOT, the software adopted from the classic BHME algorithm by Philip Laven, available at <http://www.philiplaven.com/mieplot.htm>.

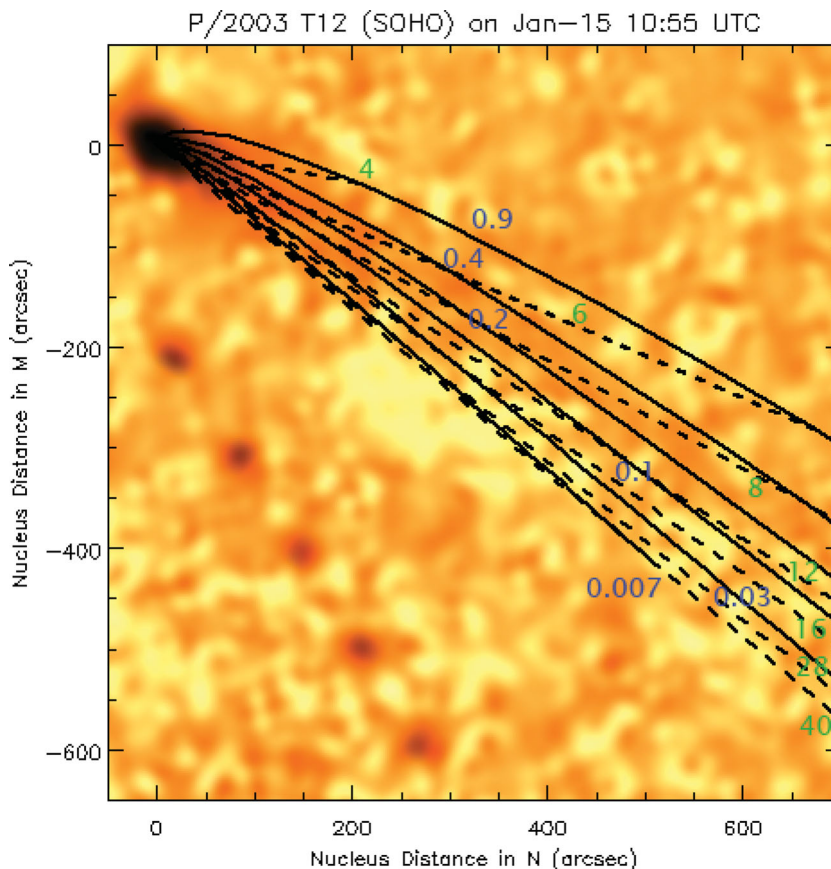


Figure 10. Comet P/2003 T12 around 11 UT on 2012 January 15 compared with the syndyne and synchrone models. The comet image was stacked with 10 neighbouring images, on average. The violet numbers label syndynes with different β values, whilst the emerald numbers label synchrones with the ejection numbers of days ahead of the observed time.

upon the uncertainties of the orbital elements, although astrometric data from ground-based observatories are not abundant. It might also suggest that a new value of g_f should be applied under the extremely large phase angle that Comet P/2003 T12 has achieved.

5 FUTURE PROSPECTS

We would encourage observations of Comet P/2003 T12 at larger r to see whether it is a more evolved comet (almost out of gas) or whether its surface would look different from other short-periodic comets or near-Earth objects. Unfortunately, it is unlikely that the comet will be observed in the next two apparitions in 2016 and 2020 around perihelion from ground-based observatories, because the viewing geometry will be excessively poor and the comet will basically remain very adjacent to the Sun. The ground-based perspective of the 2024 apparition pre-perihelion will be slightly better, but still somewhat inferior to the condition in the 2012 apparition post-perihelion. In 2028, we will witness the best ground-based observing condition of the comet in the near future, prior to perihelion, because the comet will pass by the Earth at a distance of $\Delta \sim 0.3$ au in mid-July with a relatively large elongation over 70° . Observatories situated in the Northern hemisphere will be more suitable for observations of the comet.

We have also applied the JPL HORIZONS system to check the prospects from *STEREO-A* and *STEREO-B*. However, the reality depends upon how long the twin spacecrafts continue to operate, which is less and less likely the further into the future we look.

We were delighted to see that observations from *STEREO-A* of the 2016 apparition of the comet will strikingly resemble the viewing conditions for *STEREO-B* of the 2012 apparition, yet reversing the order (i.e. the comet will make its debut in the FOV of the HI-1 camera, then proceed to and transit the FOV of the COR-2 camera). The comet is predicted to experience significant forward-scattering enhancement again, viewed from *STEREO-A*, because α_{\max} should be slightly over 175° around 2016 February 22.0 UT. Thereby, it will provide further precious opportunities to review this paper, to obtain polarimetric observations at smaller α , yet in unobserved ranges, and even to study any potential new optical phenomena of this comet at an extreme phase angle. Unfortunately, however, this is very likely the last chance to study this comet at such an extreme perspective, because in further future apparitions α will be considerably smaller. Thus, there will be no, or very limited, forward-scattering enhancement in the brightness of the comet from the views of *STEREO-A* and *STEREO-B*.

6 SUMMARY

In this work, we have investigated the light curve and polarization of Comet P/2003 T12 = 2012 A3 (*SOHO*) as photographed by the COR-2 and HI-1 cameras of *STEREO-B* in an unprecedented observed large phase angle up to 177.6° . The following results were found.

The comet was deduced to be gassy from the magnitude difference between the HI-1 and COR-2 observations.

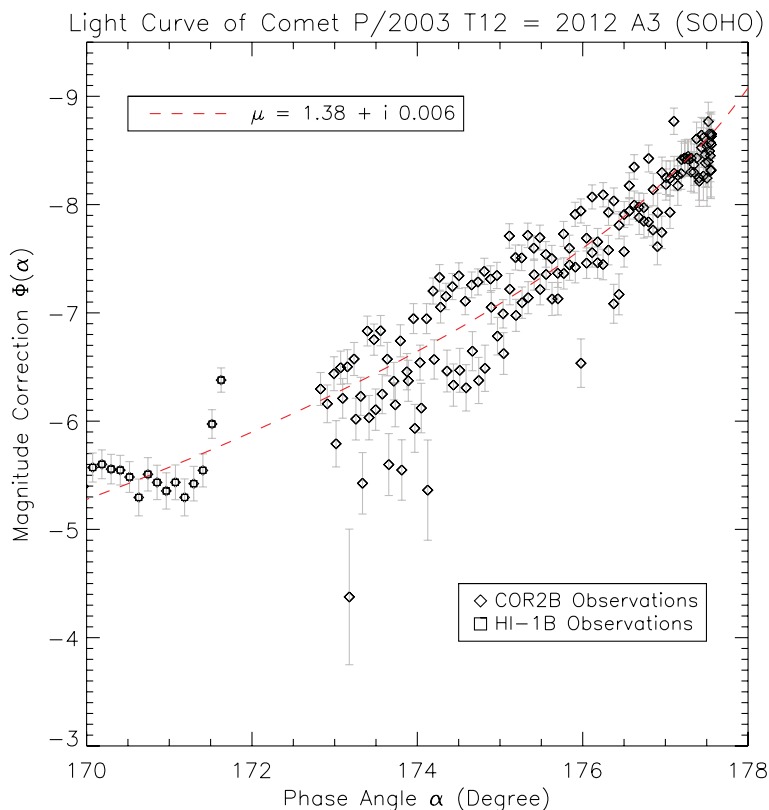


Figure 11. Theoretical best-fitting Mie scattering phase function to the COR-2 observation data.

The brightness of the comet is greatly intensified because of the forward-scattering effect, by around -8.5 mag, around $\alpha_{\max} = 177.6$. The compound HG model accurately matches the HI-1 observations in the range $129^\circ \lesssim \alpha \lesssim 172^\circ$, which, by contrast, predicts a brightening slope much gentler than the trend of the COR-2 observations in the range $173^\circ \lesssim \alpha \leq 177.6$ as α increases. It was proved that the greater steepness should not be related to the proximal tail contamination through the simplified simulation. Our analysis has revealed that it is likely that Mie scattering due to the large sizes of dust particles accounts for the steeper slope of the brightness enhancement. Mie spheres with R between 1 and 20 μm , $\mu = 1.38 + i 0.006$ and $p = 3$ could fit the COR-2 observations very well. It might also suggest a different value g_f in the compound HG model under the extreme geometry.

Polarization data of the comet were obtained, with α as great as $\alpha_{\max} = 177.6$, and thus the polarization is from the largest phase angle so far. The debiased polarization data were mainly $P \sim 0$ throughout the observed range $172.9 \leq \alpha \leq \alpha_{\max}$. The data do not illustrate convincing temporal variations of the polarization either. Given the errors, the data confirm the computer modelling results of scattered light due to large aggregates by Kolokolova & Mackowski (2012).

ACKNOWLEDGEMENTS

This work concerning Comet P/2003 T12 has received much help of great value from Joseph N. Marcus and Matthew M. Knight, to whom we are most indebted. We appreciate Steve Larson for granting the permission to use the spectrum of Comet 8P/Tuttle, and we thank Angelos Vourlidas for sending his measurement of the COR-2 effective transmission. We thank the whole STEREO team

for making the data used here available to the public. We are also grateful to William T. Thompson, Angelos Vourlidas, David Jewitt and an anonymous referee for their valuable comments, discussions and correspondence concerning the manuscript.

REFERENCES

- Bewsher D., Brown D. S., Eyles C. J., Kellett B. J., White G. J., Swinyard B., 2010, *Solar Phys.*, 264, 433
 Bewsher D., Brown D. S., Eyles C. J., 2012, *Solar Phys.*, 276, 491
 Eyles C. J. et al., 2009, *Solar Phys.*, 254, 387
 Fulle M., 2004, in Festou M. C., Keller H. U., Weaver H. A., eds, *Comets II*. University of Arizona Press, Tucson, AZ, p. 565
 Grynko Y., Jockers K., Schwenn R., 2004, *A&A*, 427, 755
 Howard R. A. et al., 2008, *Space Sci. Rev.*, 136, 67
 Jewitt D., Meech K. J., 1986, *AJ*, 310, 937
 Kaiser M. K., Kucera T. A., Davila J. M., St.Cyr O. C., Guhathakurta M., Christian E., 2008, *Space Sci. Rev.*, 136, 5
 Knight M. M., A'Hearn M. F., Biesecker D. A., Faury G., Hamilton D. P., 2010, *AJ*, 139, 926
 Kolokolova L., Mackowski D., 2012, *J. Quant. Spectrosc. Radiat. Transf.*, 113, 2567
 Marcus J. N., 2007a, *Int. Comet Quarterly*, 29, 39
 Marcus J. N., 2007b, *Int. Comet Quarterly*, 29, 119
 Marsden B. G., Kisala R., Battsams K., 2004, *Minor Planet Electronic Circ.*, 2004-K33
 Pickles A. J., 1998, *PASP*, 110, 863
 Sato H., Williams G. V., 2012, *Minor Planet Electronic Circ.*, 2012-B111
 Wardle J. F. C., Kronberg P. P., 1974, *AJ*, 194, 294
 Williams G. V., Battsams K., 2012, *Minor Planet Electronic Circ.*, 2012-B96.